TECHNICAL MEMORANDUM

53

An evaluation of three ten day forecasts for the Australian region during FGGE SOP 2

M. Vaughn

Research Department

February 1982

European Centre for Medium-Range Weather Forecasts
Europäisches Zentrum für mittelfristige Wettervorhersage
Centre européen pour les prévisions météorologiques à moyen

1. INTRODUCTION

This study is a result of an informally arranged joint project between Dr. W. Bourke, ANMRC and Dr. D. Burridge, ECMWF. The period 17-28 May 1979 during FGGE SOP-2 is of particular interest to ANMRC because of the cyclogenesis in Western Australia accompanying a cold outbreak. Three forecast experiments were made at ECMWF - E89 a ten day forecast beginning on 20 May, E90 a ten day forecast beginning on 22 May and E91 a ten day forecast beginning on 24 May. All three experiments used FGGE Level III b ECMWF analyses as initial data. ANMRC have conducted a series of numerical experiments for this period,assessing predictability and impact of observing systems in the Southern Hemisphere (Bourke, 1980).

2. SYNOPTIC EVALUATION OF THE EC-ANALYSED FGGE DATA FOR 20-28 MAY (AUSTRALIAN REGION)

Figure 1 shows the mean sea level pressure and 850 mb temperature for the EC-analyses (00Z) of the FGGE data for 20-29 May. Figure 2 shows the 500 mb height and temperature fields for the same period.

2.1 Sea level analysis

On 20 May there is a deep cold trough south of the western region of the Great Australian Bight with a strong anticyclone over eastern Australia and an anticyclone west of Australia extending into the Indian Ocean. The eastern anticyclone has a strong warm southward extension over the ocean and a cold eastward extension reaching as far as New Zealand over the Tasman Sea. By 21 May the trough has developed into a low pressure system over south western Australia accompanied by an outbreak of cold air in that region. The low further intensifies by 22 May when it is situated over the Great Australian Bight, the eastern anticyclone remaining fairly stationary over the Tasman Sea. On 23 May the low weakens, moves south and then east over the next two days accompanied by a weakening of the eastern anticyclone which is however re-established over eastern Australia by 25 May. The cooling in

the western region continues on 23 May and a new low pressure area develops into a new cold trough by the 24th. The trough gradually moves south eastwards until it reaches south eastern Australia on 27 May with the western anticyclone reestablished inland. By 28 May the warm anticyclone has essentially been re-established over most of Australia.

A notable feature during this period is the cold trough north west of New Zealand on 22 May. This develops into an intense cyclone north of New Zealand on 24 May and subsequently moves south eastwards, weakening.

2.2 500 mb analyses

The 500 mb flow pattern reflects the surface analyses. On the 20th May the 500 mb analysis shows a strong cold trough aloft situated directly above the surface trough to the SW of Australia and a somewhat weaker trough to the east over New Zealand associated with a region of cold air to the north of New Zealand. Connecting these two troughs is a strong warm ridge south of Tasmania. This ridge deepens in a south easterly direction by the following day as the western trough moves further north over western Australia in conjunction with the movement of the surface trough. By the 22nd May a cold cut off low forms over the Great Australian Bight directly over the deep surface depression. This low weakens into a trough which moves rapidly south eastwards during the next few days in a similar manner to the surface low.

Meanwhile, by the 23rd, the western part of the trough expands over Western Australia with cyclogenesis occurring in the south west on the 25th May directly over the pool of cold air at the surface behind the new surface trough. This depression weakens into a trough and moves south eastwards over the Great Australian Bight on the 26th May with essentially zonal flow established over Australia by the 28th May.

On the 21st May the eastern trough deepens and develops an orientation towards the northwest. A cut off low forms on the 23rd, a day ahead of the surface cyclone north of New Zealand. The trough remains in this region gradually warming until the 27th when it starts to fill and moves eastwards.

3. SUBJECTIVE COMPARISONS (AUSTRALIAN REGION) OF E89,E90 and E91

3.1 Synoptic description of E89

Figure 3 shows the mean sea level pressure and the 850 mb temperature for the ten day forecast E89 starting on 20 May 1979. Figure 4 shows the 500 mb height and temperature fields for E89.

The cold deep trough to the south west of Australia on 20 May is incorrectly forecast to weaken on the 21st with a pressure gradient that is too weak and become a general area of low pressure in mid Australia on the 22nd thus missing the development of the deep low in the Bight on 22 May. The cold outbreak in the south western region is well forecast however for the 21st and correctly maintained in the region until the 26th. At 500 mb the western and eastern troughs and connecting ridges deepen and move in the right directions on the 21st but the western trough fails to develop the cut-off low in the Bight on the 22nd whereas in the eastern trough a cut off low develops a day early to the north west of New Zealand.

At the surface on 23 May the low pressure area in mid Australia is forecast to develop into a weak low pressure system over the Bight which is then forecast to move slowly eastwards to reach Tasmania on the 25th displacing the eastern anticyclone further east with the western anticyclone re-establishing the anticyclonic circulation over S.W. Australia. The forecast fails to develop a trough at the surface in western Australia on the 24th. At 500 mb the troughs maintain good positions until they near the end of the forecast on the 29th May but cyclogenesis fails to occur in the western trough on the 25th.

At the surface a trough is forecast on the 3rd day north west of New Zealand which is correctly developed into the deep depression north of New Zealand on the 4th day of the forecast and moves south eastwards decaying on the 7th day.

3.2 Synoptic description of E90

Figure 5 shows the mean sea level pressure and the 850 mb temperature for the ten day forecast E90 starting on 22 May 1979. Figure 6 shows the 500 mb height and temperature fields for E90.

The forecast E90 starts with the deep depression at the surface in the Bight on 22 May. This low is forecast correctly to weaken and move south on the 23rd and then eastwards as a trough on the 24th and 25th losing amplitude with the eastern anticyclone moving north eastwards over eastern Australia. The cold trough correctly forms over western Australia on the 24th and is forecast to develop into a new low in the Bight on 26 May instead of the weak low in the analysis. The depression is then forecast to move eastward over Tasmania by the 28th whereas the trough in the analysis reaches this position by the 27th. The western antidepression correctly moves eastward behind the depression to re-establish the anticyclonic circulation over Australia. The cold trough north west of New Zealand on the 22nd correctly develops into a strong depression north of New Zealand by the 24th and subsequently moves south eastwards into the Pacific Ocean.

At 500 mb the position and amplitudes of both the eastern and western troughs and the connecting ridge are very well forecast for the first four days. Cyclogenesis is correctly forecast at 24 hours in the eastern trough to the northwest of New Zealand on the 23rd May and in the western trough on the 25th May. Zonal flow is correctly established at 500 mb over Australia on 28th May the sixth day of the forecast

3.3 Synoptic description of E91

Figure 7 shows the mean sea level pressure and the 850 mb temperature for the ten day forecast E91 starting on 24 May 1979. Figure 8 shows the 500 mb height and temperature fields for E91.

The forecast E91 starts with the new cold trough at the surface situated over western Australia between the two southward extending warm anticyclones, one over eastern Australia and the Tasman Sea, the other west of Australia in the Indian Ocean. The deep low is already developed north of New Zealand.

The trough is correctly forecast to move south eastwards into the Great Australian Bight on the 25th and then to weaken into a general low pressure area over Melbourne and Tasmania on the 26th, a position about 8° too far east. On the 27th the low pressure area is forecast to develop into a trough off the east coast of Australia which compares quite well with the analysis but the gradient is too weak.

As the surface trough moves south eastwards the two anticyclones are correctly forecast to move northwards and closer together. The cold outbreak in the south west persists as it should until the 26th when it then disperses.

The cyclone north of New Zealand moves correctly to the south east gradually filling over a period of three days somewhat more slowly than the analysis.

At 500 mb the position of the eastern and western trough and connecting ridge are correctly forecast until zonal flow is established over Australia on the 27th May. However, the forecast fails to develop a cut-off low in the western trough on 25th May.

3.4 Subjective comparisons

E90 is the most successful of the three forecasts in the Australian region since it correctly forecasts the southward movement and decay of the first surface low from the Great Australian Bight and the movement of the eastern anticyclone back over eastern Australia. At 500 mb the cyclogenesis in both the eastern and western troughs is well forecast on the first and third days respectively of the forecast. The western cold trough at the surface is also well developed until the 4th day of the forecast and correctly moved to the southeast with the western anticyclone re-establishing the anticyclonic circulation behind it.

E91 is a good forecast too compared with E89 which failed to develop the low in the Bight on 22nd May.

The 850 mb and 500 mb temperature is very well forecast in all three experiments for the Australian and New Zealand region. In each of the experiments the cold outbreak in western Australia and to the northwest of New Zealand is well forecast and correctly maintained until 26 May.

The development and decay of the deep low north of New Zealand is an exceptional feature of the forecast in all three experiments, particularly in E89 where the depression is forecast for the 4th day and is correctly maintained until its decay on the 7th day.

4. OBJECTIVE COMPARISONS

For objective evaluations of the forecast the most commonly used objective skill scores, viz. the standard deviations and correlation coefficients are available for the whole Southern Hemisphere only. Since insufficient climatological data is available for the Southern Hemisphere the standard deviations from the climatological mean (called NORM) have not been calculated.

4.1 Verification of the height fields

4.1.1 Standard deviation of height scores

Figures 9, 10 and 11 show the mean standard deviations of the 500 mb height field for each of the experiments E89, E90 and E91 for the area between 20° south and 82.5° south. The top panels give the values for the total field and the lower panels show the contributions by different scales of motion to the total standard deviation.

The error growth rate in all three experiments is very similar gradually reaching 120 m at 7 days. (Note that E91 is verified over a shorter period than E89 and E90 due to lack of verifying data). The persistence forecast shows a strong increase in error during the first twelve hours in all panels which is considered to be due to the level of uncertainty in the analysis (Arpe, 1981). In all three forecasts the main advantage over persistence is to be found in the medium waves (wavenumbers 4 to 9) lasting for about 4 to 5 days.

4.1.2 Anomaly correlation coefficients of height

The anomaly correlation coefficients of the 500 mb height field give a measure of the predictability of the forecast in the Southern Hemisphere where normally the 60% intersection of the anomaly correlation coefficients is considered as the limit of acceptability. Figures 12, 13 and 14 show the anomaly correlation coefficients for experiments E89, E90 and E91 for the total fields and the long, medium short wave and zonal components. E91 has the highest predictability taking 5.5 days to reach the 60% level which compares favourably with ECMWF Northern Hemispheric experiments in early winter. The limit of predictability is 5 days for E89 and E90. In all three experiments the predictability is highest for the long waves which reach the 60% limit at 5.8, 5.5 and 5 days for E91, E89 and E90 respectively. Predictability for the medium waves is 5, 4.2 and 3.7 days respectively. The

zonal component for each forecast shows no advantage over the persistence forecast.

The predictability decreases with height (figures not shown) since the time taken for the anomaly correlation coefficients of the 1000 mb height fields to intersect the 60% level is 4.3, 3.9 and 3.9 for E91, E89 and E90 respectively. Again, the predictability is highest for the long waves.

4.2 Verification of the temperature fields

4.2.1 Standard deviations

Figures 15, 16 and 17 show the standard deviations of the 850 mb temperature fields for each of the forecasts E89, E90 and E91. Both the forecasts and the persistence forecast show a high initial error growth to the level of between 2 and 3K. In a previous study (Arpe, 1981) of Southern Hemisphere forecasts made at ECMWF this was found to be the level of the uncertainty between ECMWF and NMC analyses for the period under study.

The forecasts show some improvement over persistence for four to five days mainly due to the contribution from the medium waves (wavenumbers 4 to 9) and long wages (wavenumbers 1 to 3) but the zonal and short wave components show hardly any skill at all. The standard deviations of the zonal mean fields show a diurnal variability which was also apparent (Arpe, 1981) between the ECMWF and NMC analyses. Since the persistence forecast and the operational forecast only showed diurnal variability in comparison with EC-analyses it was then considered that the diurnal variability was in the EC Southern Hemisphere analyses scheme.

4.2.2 Anomaly correlation coefficients

The anomaly correlation coefficients of the 850 mb temperature fields (Figs. 18, 19 and 20) show E89, E90 and E91 reaching the 60% predictability limit at days 4.4, 3.4 and 3.7 respectively. The predictability is again highest for the long waves which reach the 60% limit at 4.6, 5.0 and 3.2 days respectively.

5. CONCLUSIONS

The objective scores at 500 mb show that experiment E91 has the highest predictability of 5.5 days in the height field for the complete Southern Hemisphere region followed by E89 and E90 at 5 days. The temperature predictability is highest for E89 with a limit of 4.4 days for the Southern Hemisphere region. Figs. 21, 22 and 23 show the 500 mb height and temperature fields for each of the forecasts compared with the analyses at days 4 and 5 in support of these conclusions.

The performance of these forecasts is comparable with Northern Hemisphere results for late Autumn forecasts and demonstrate the ability of the ECMWF model to make good medium range forecasts in the Southern Hemisphere given a data base of the quality of FGGE data.

REFERENCES

Arpe, K. 1981 Performance of the ECMWF Forecasts at the Southern Hemisphere. Personal communication.

Bourke, W. Seaman,R. and Puri,K 1980 Assimilation Analysis, Prognosis and Data Impact in Southern Hemisphere during SOP-2. International Conference on Preliminary FGGE Data Analysis and Results (Bergen, Norway, 23-27 June 1980). WMO,ICSU.

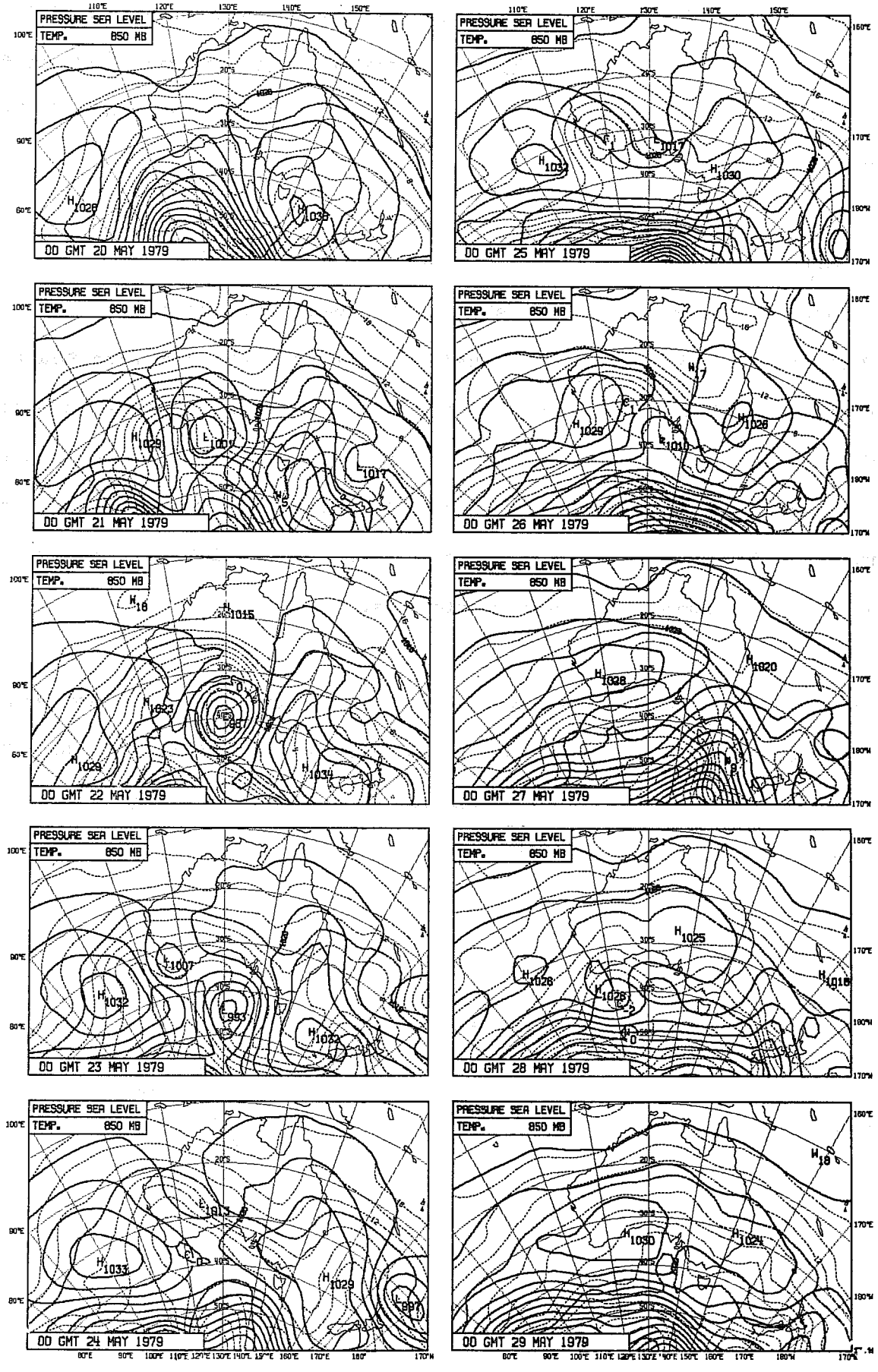

Fig. 1 EC analysed mean sea level pressure and 850 mb. temperature

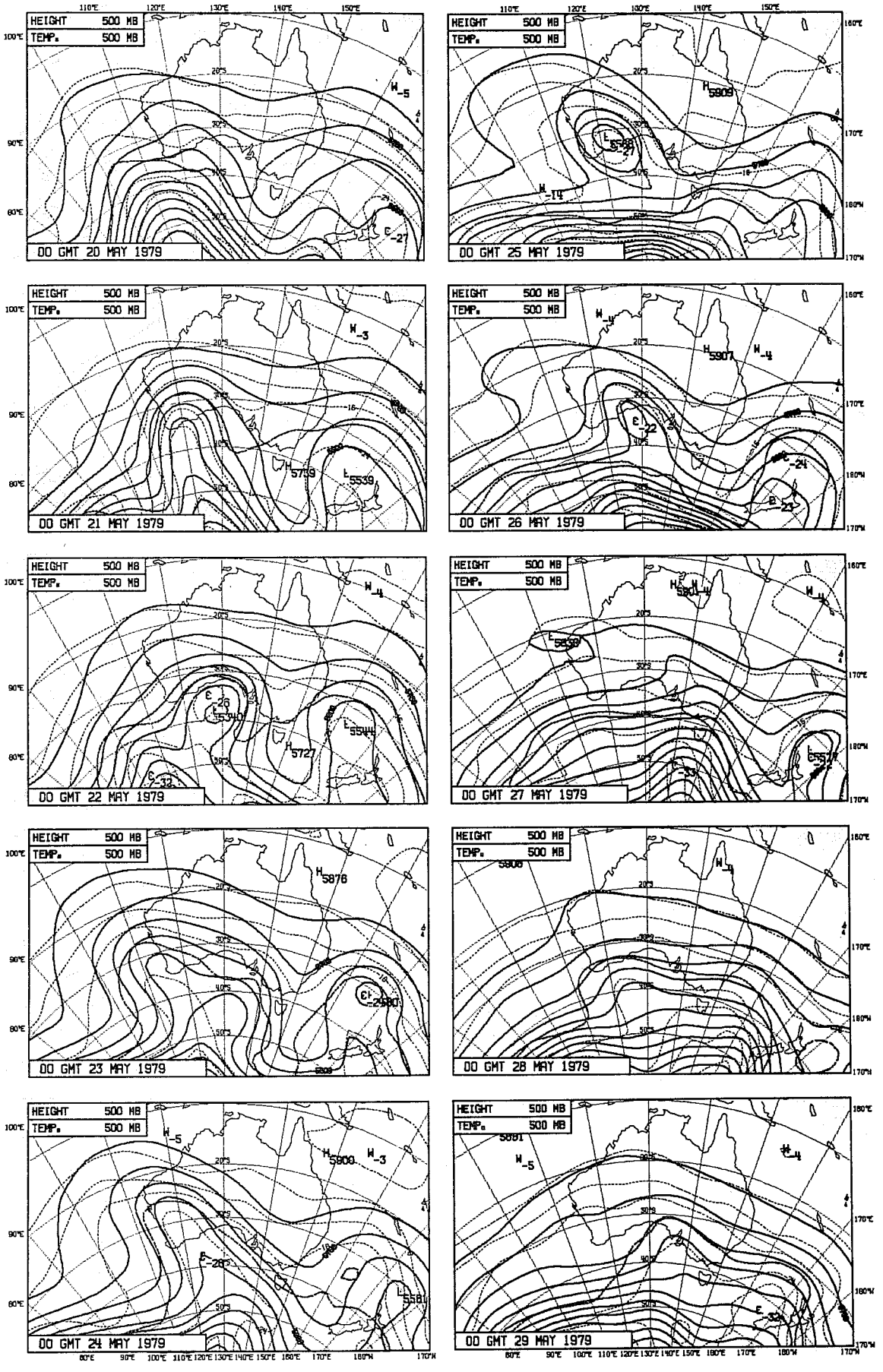

Fig. 2 EC analysed 500 mb. height and 500 mb. temperature

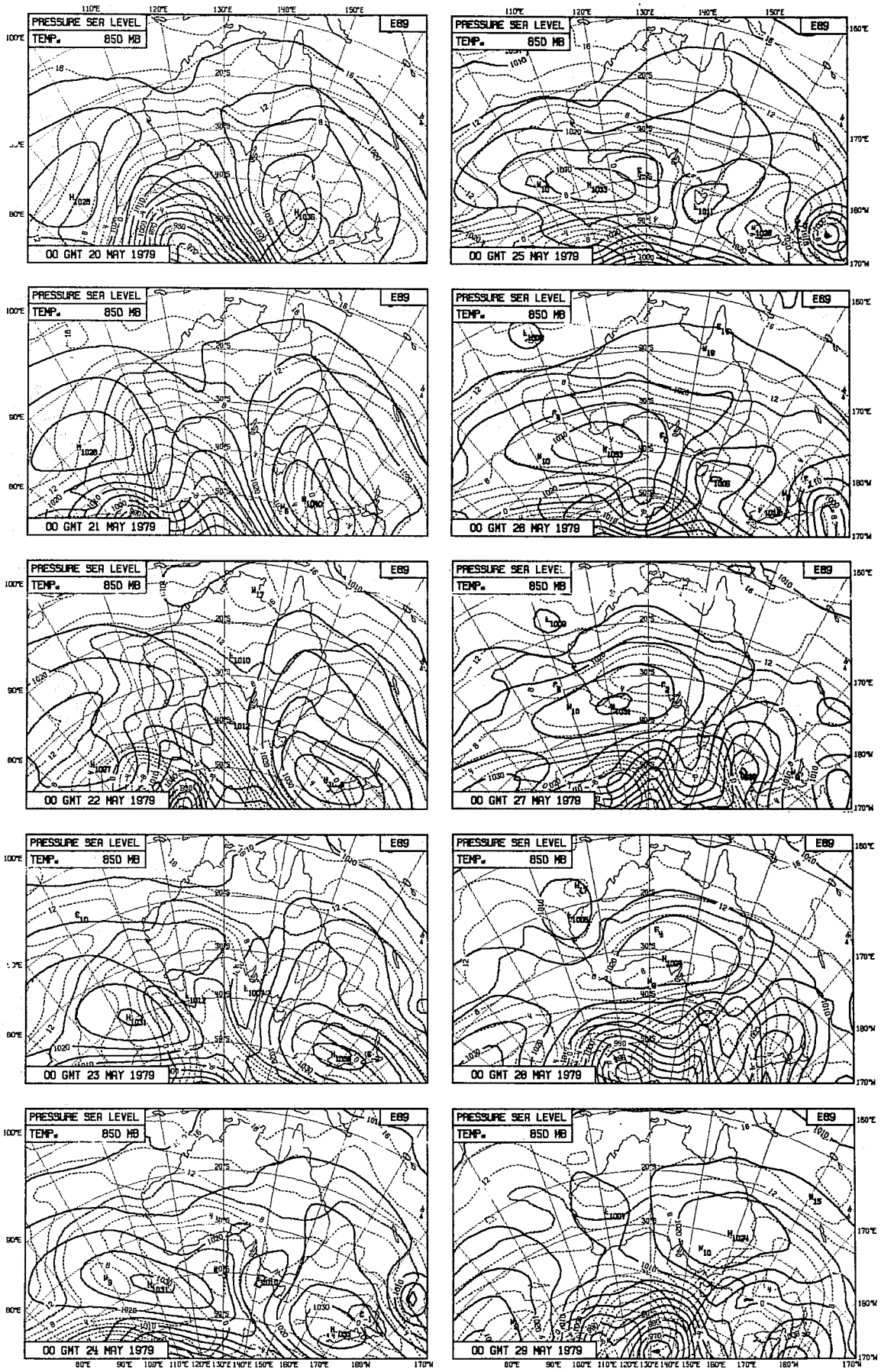

Fig. 3 Forecast E89 mean sea level pressure, 850 mb. temperature

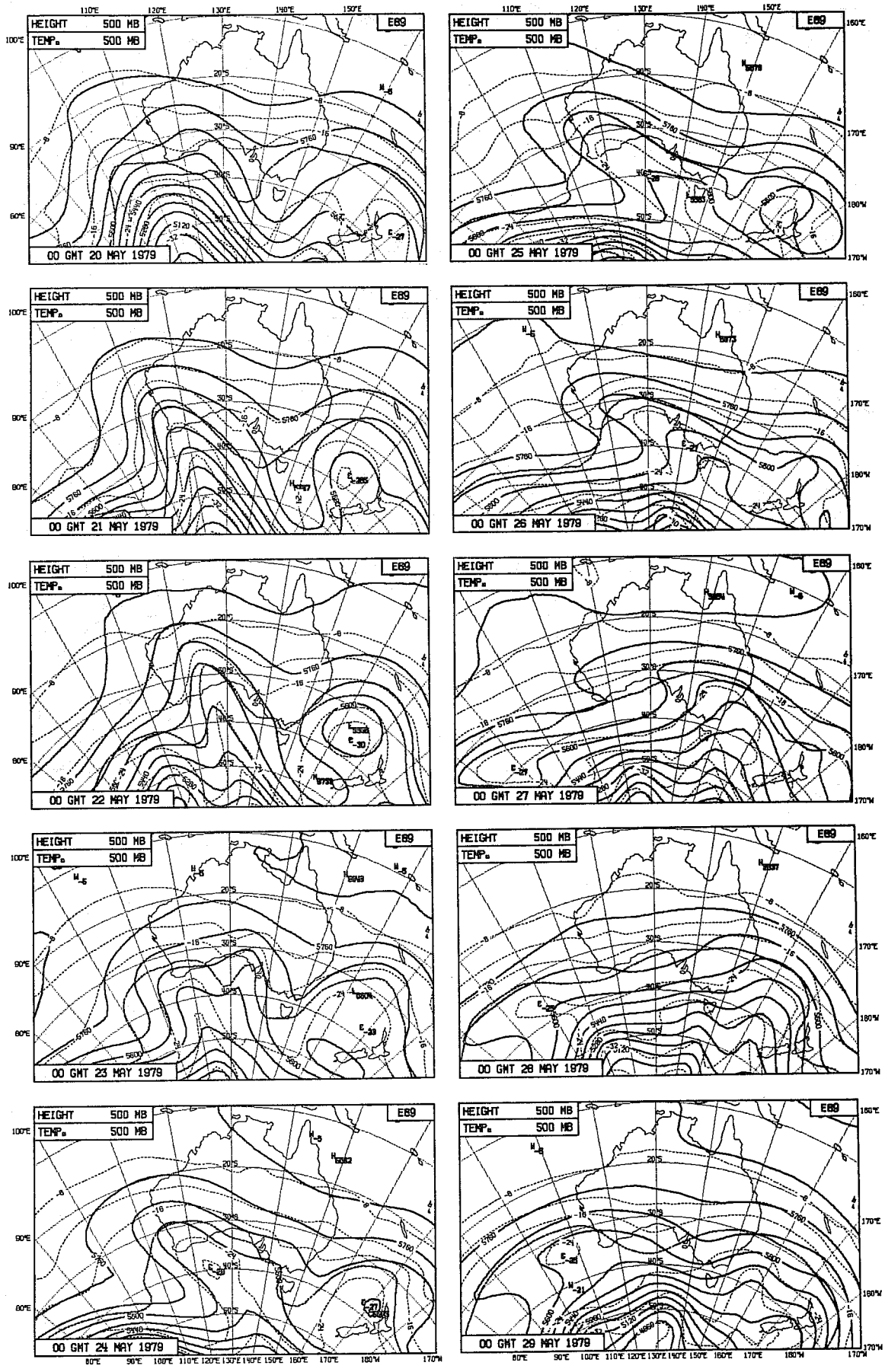

Fig. 4 Forecast E89 500 mb. height and 500 mb. temperature

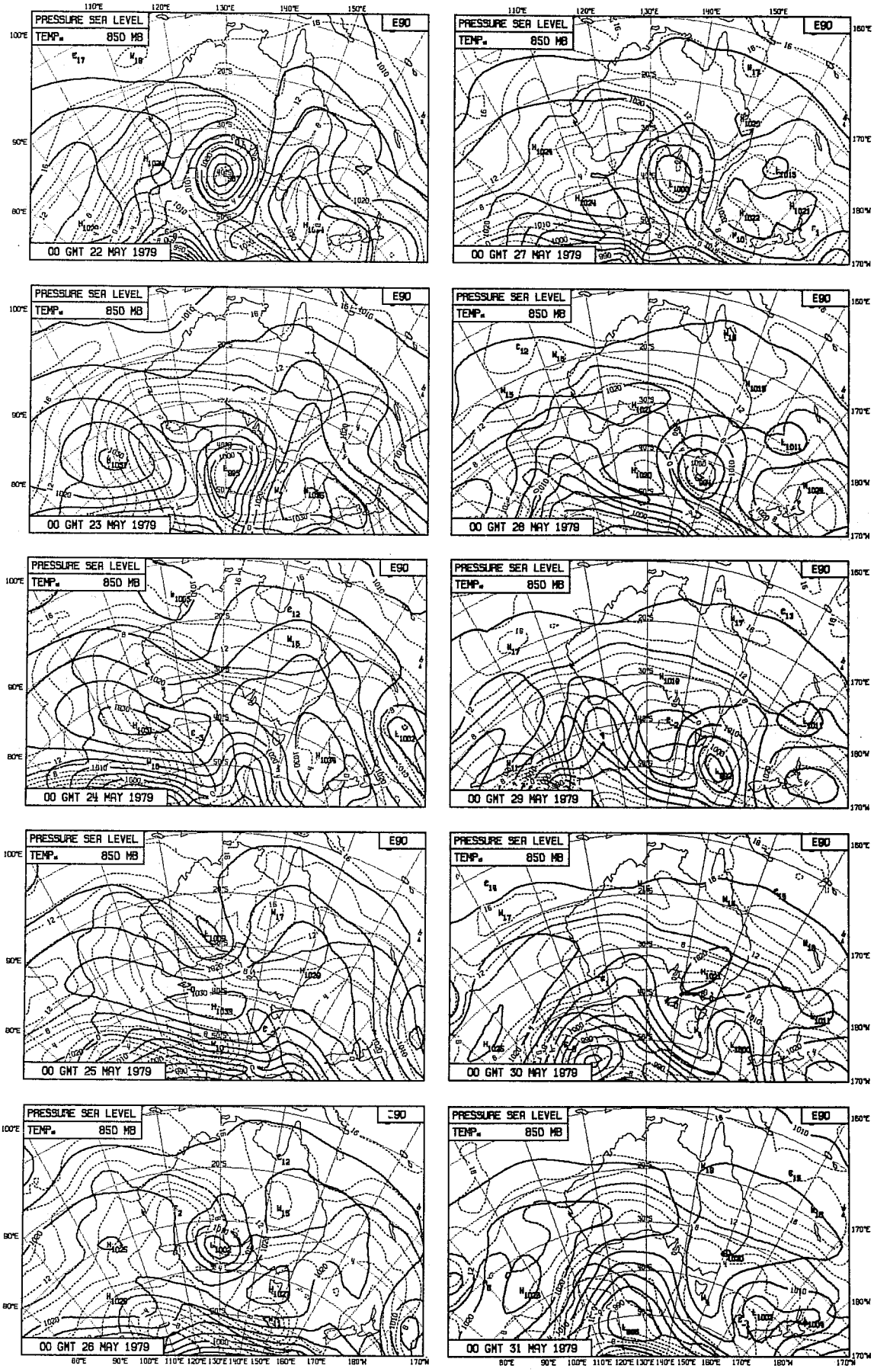

Fig. 5 Forecast E90 mean sea level pressure, 850 mb. temperature

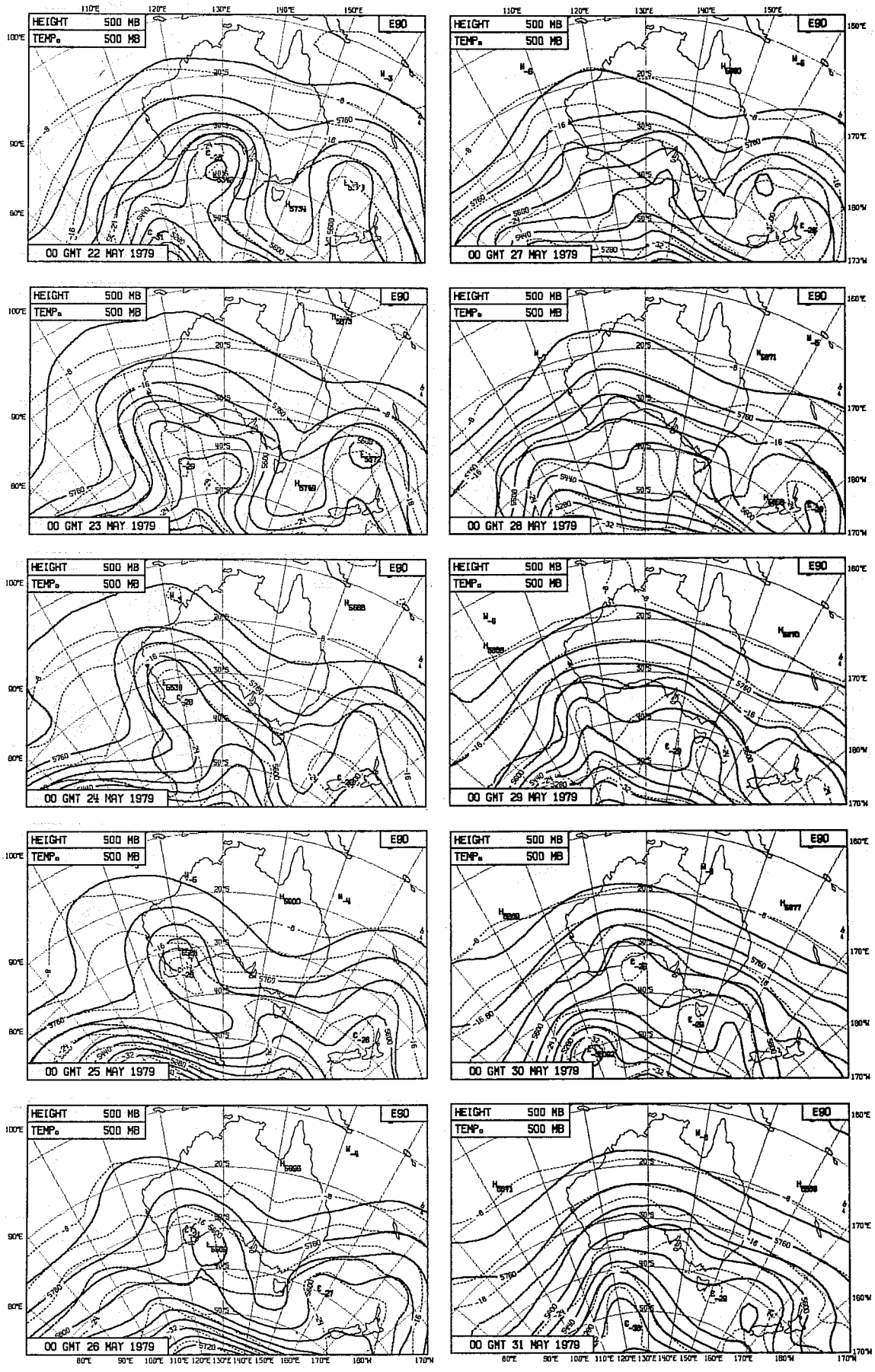

Fig. 6 Forecast E90 500 mb height and 500 mb. temperature

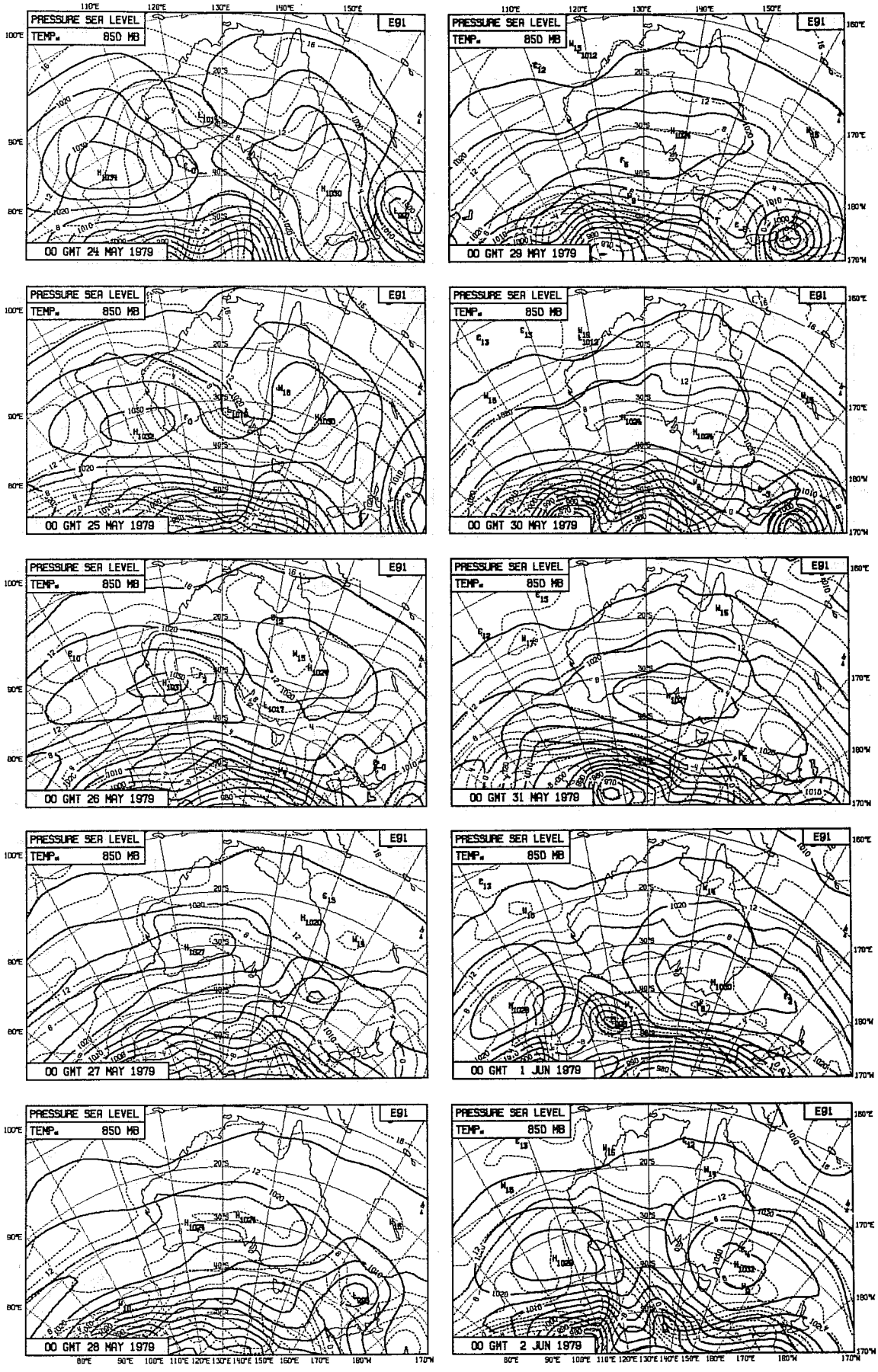

Fig. 7 Forecast E91 mean sea level pressure, 850 mb. temperature

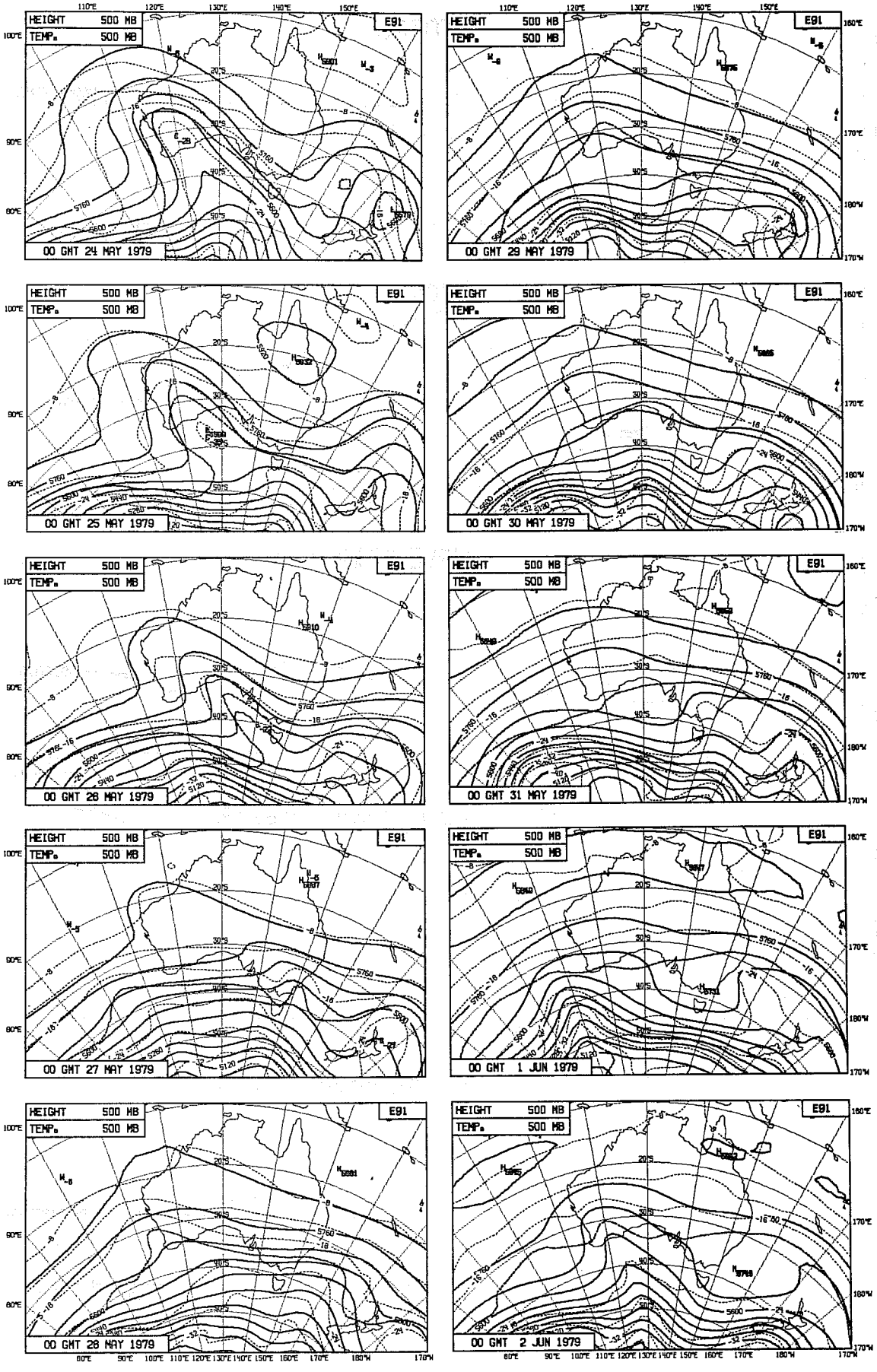

Fig. 8 Forecast E91 500 mb. height and 500 mb. temperature

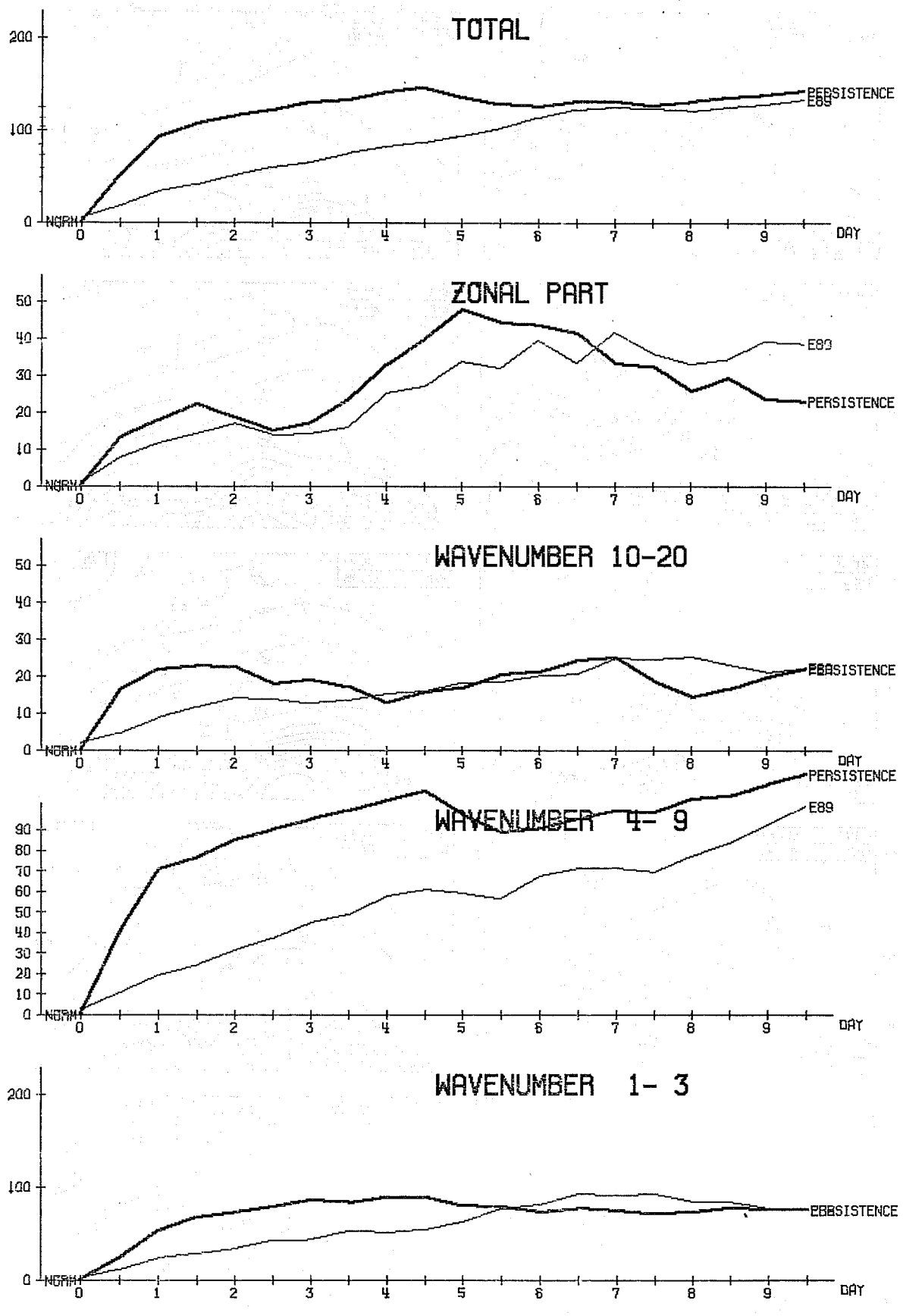

Fig. 9 E89 Mean standard deviation of 500 mb. height fields

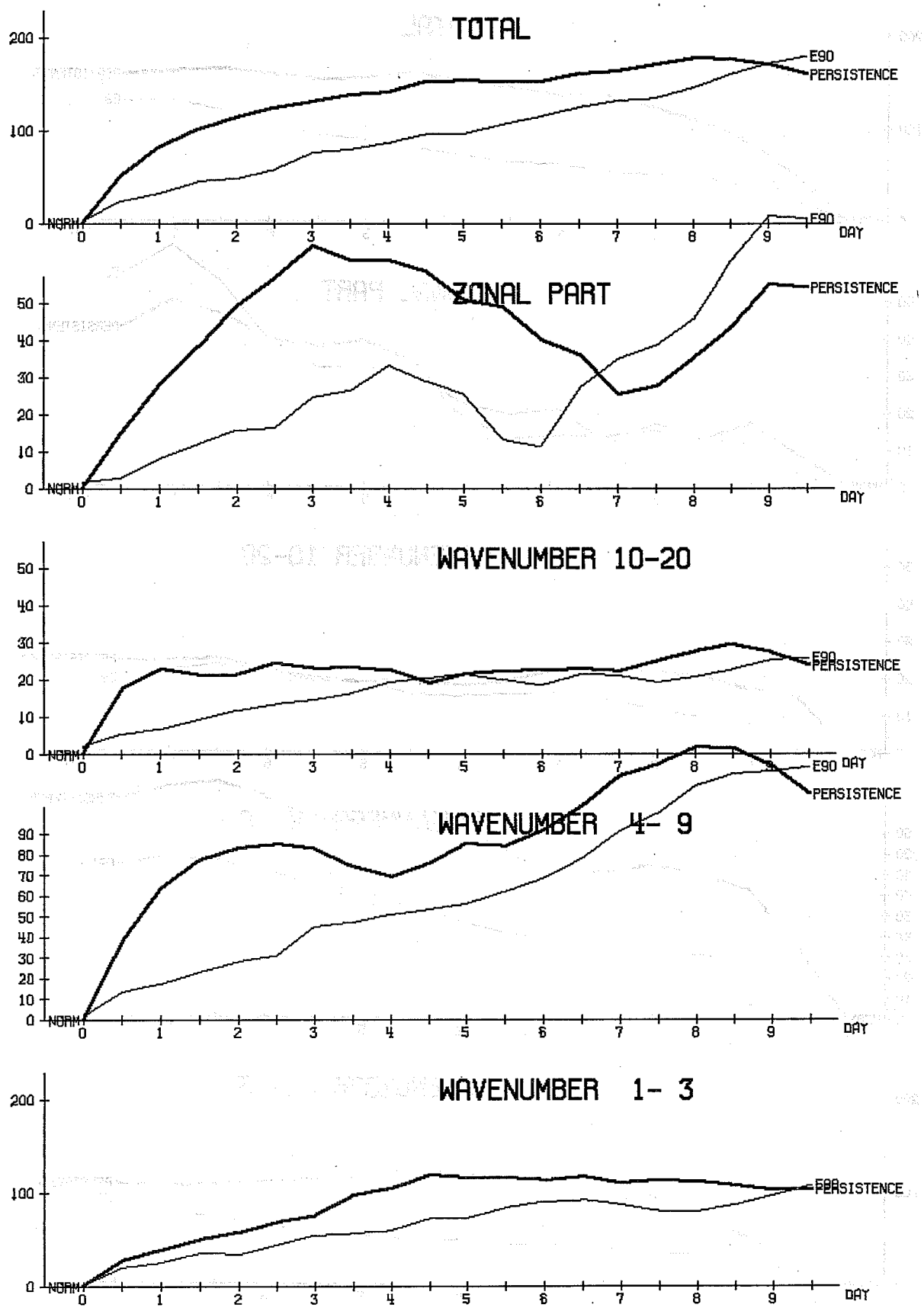

Fig. 10 E90 Mean standard deviation of 500 mb. height fields

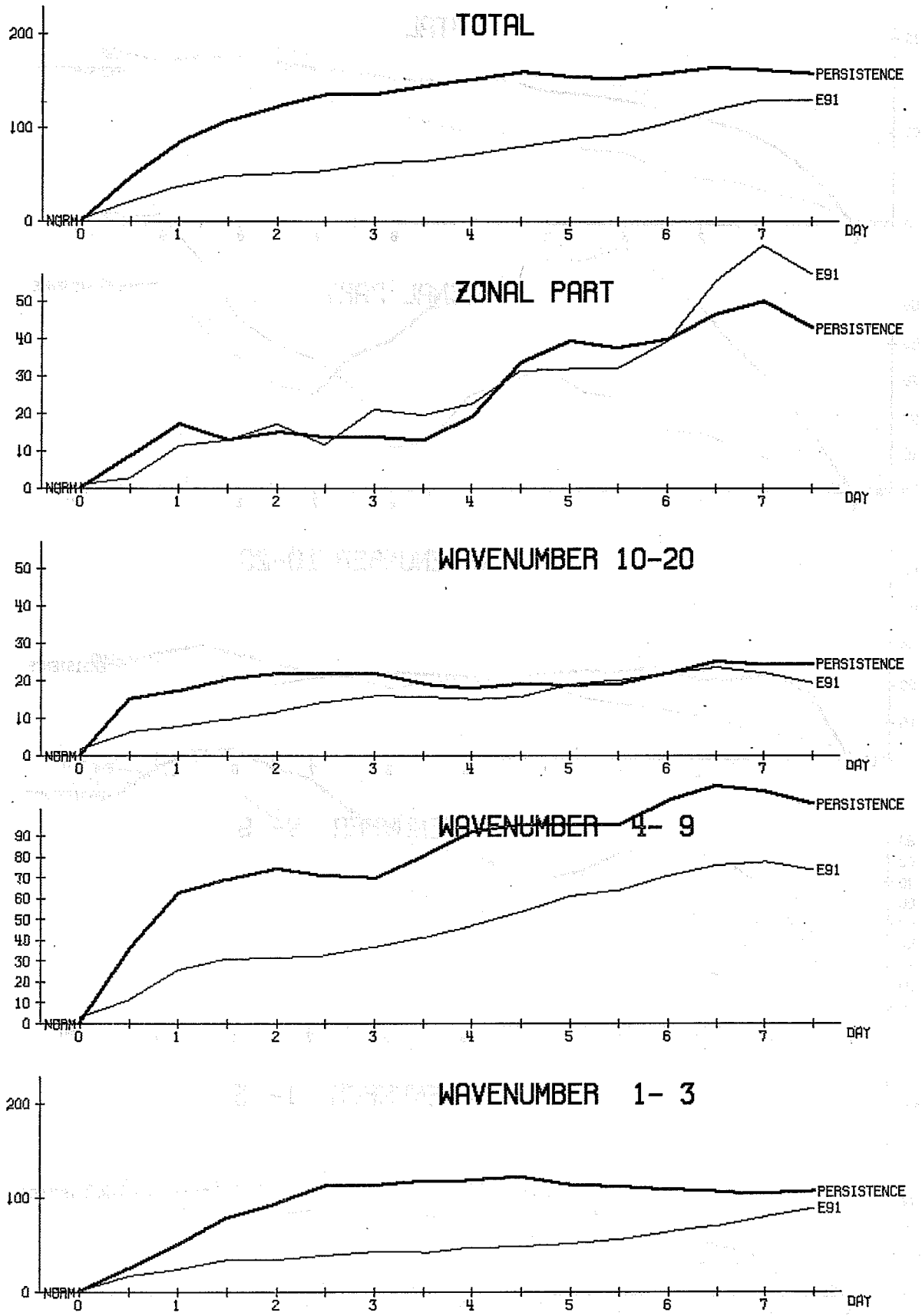

Fig. 11 E91 Mean standard deviation of 500 mb. height fields

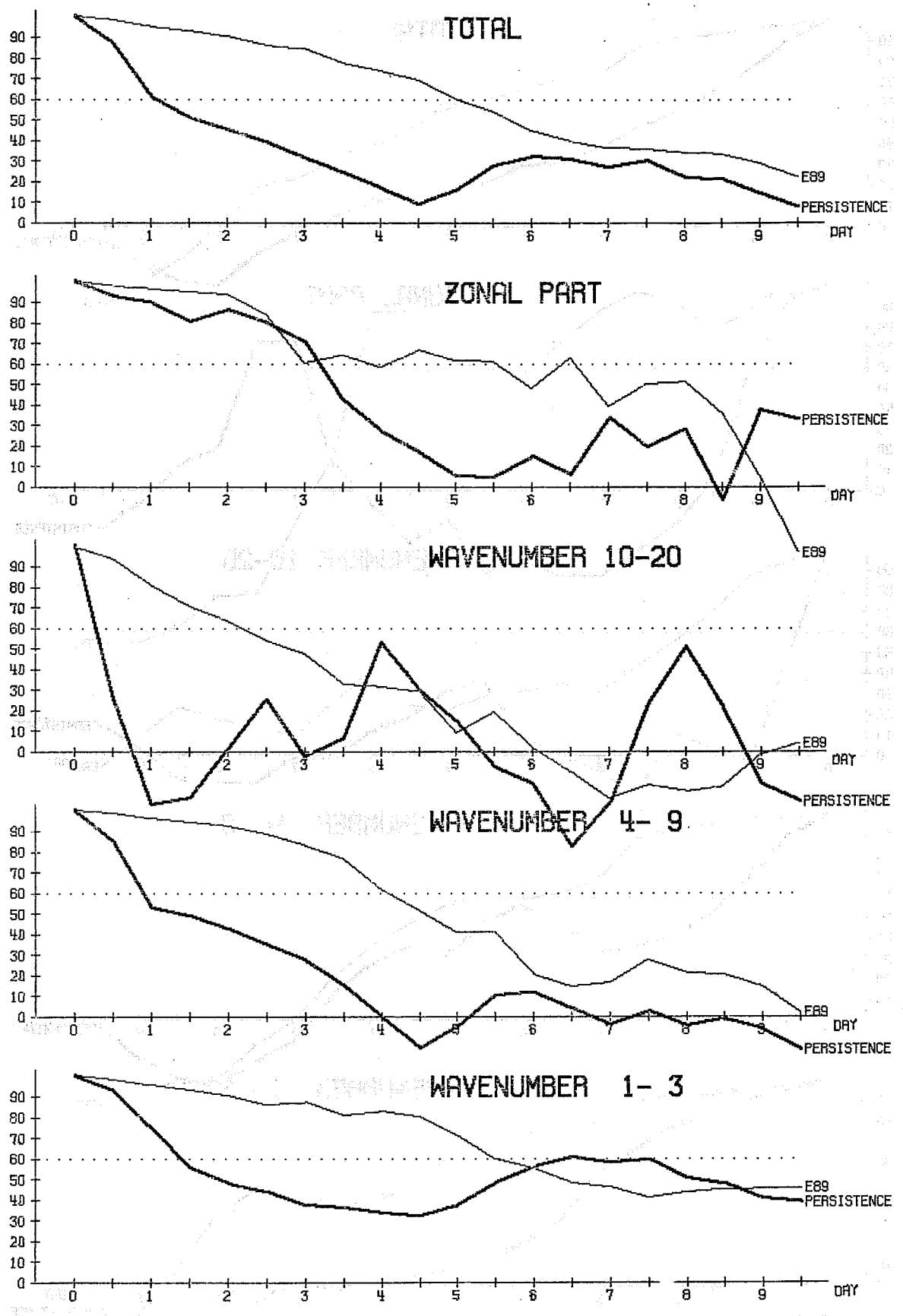

Fig. 12 E89 Anomaly correlation coefficients of the 500 mb. height fields

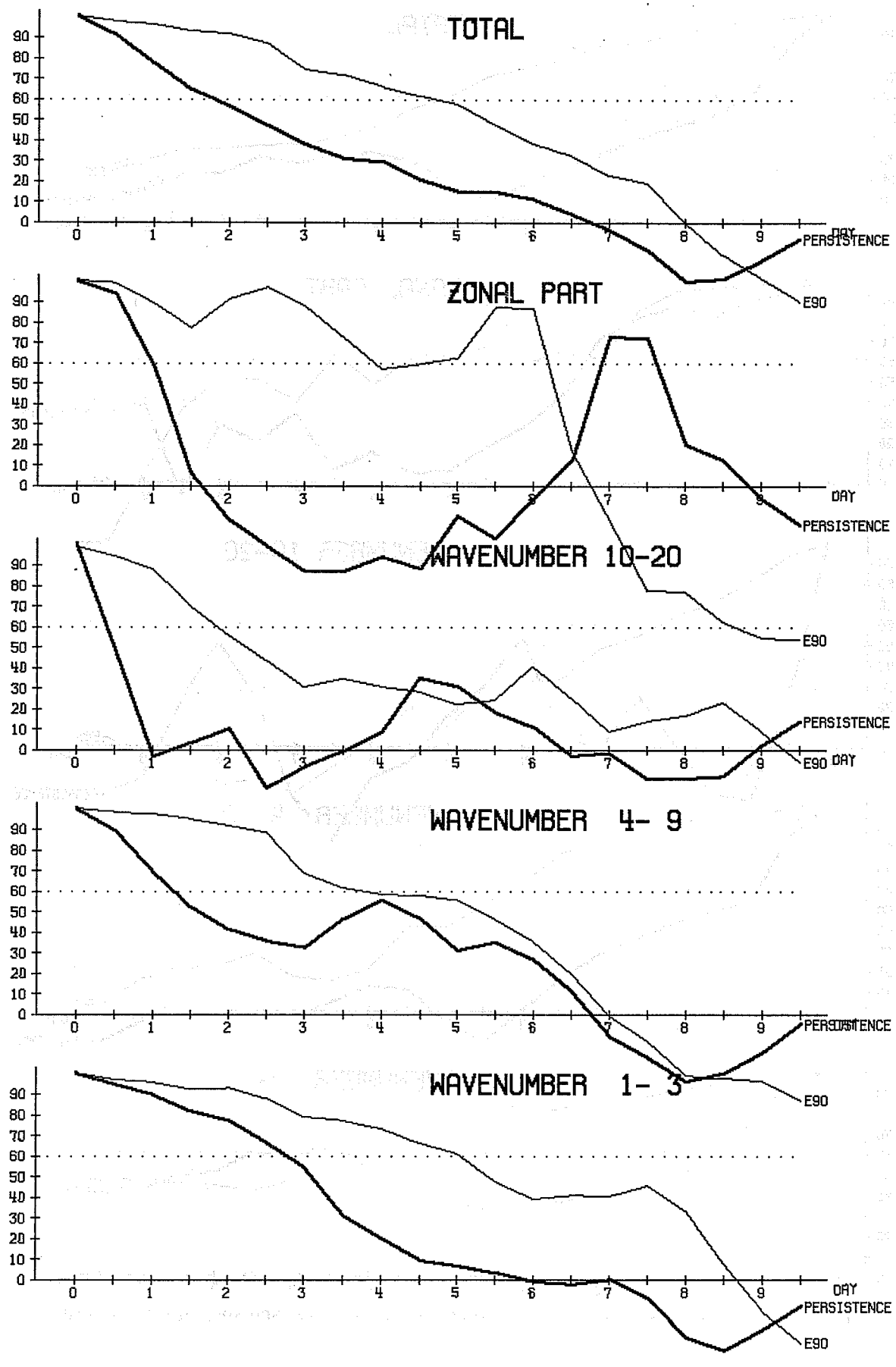

Fig. 13 E90 Anomaly correlation coefficients of the 500 mb. height fields

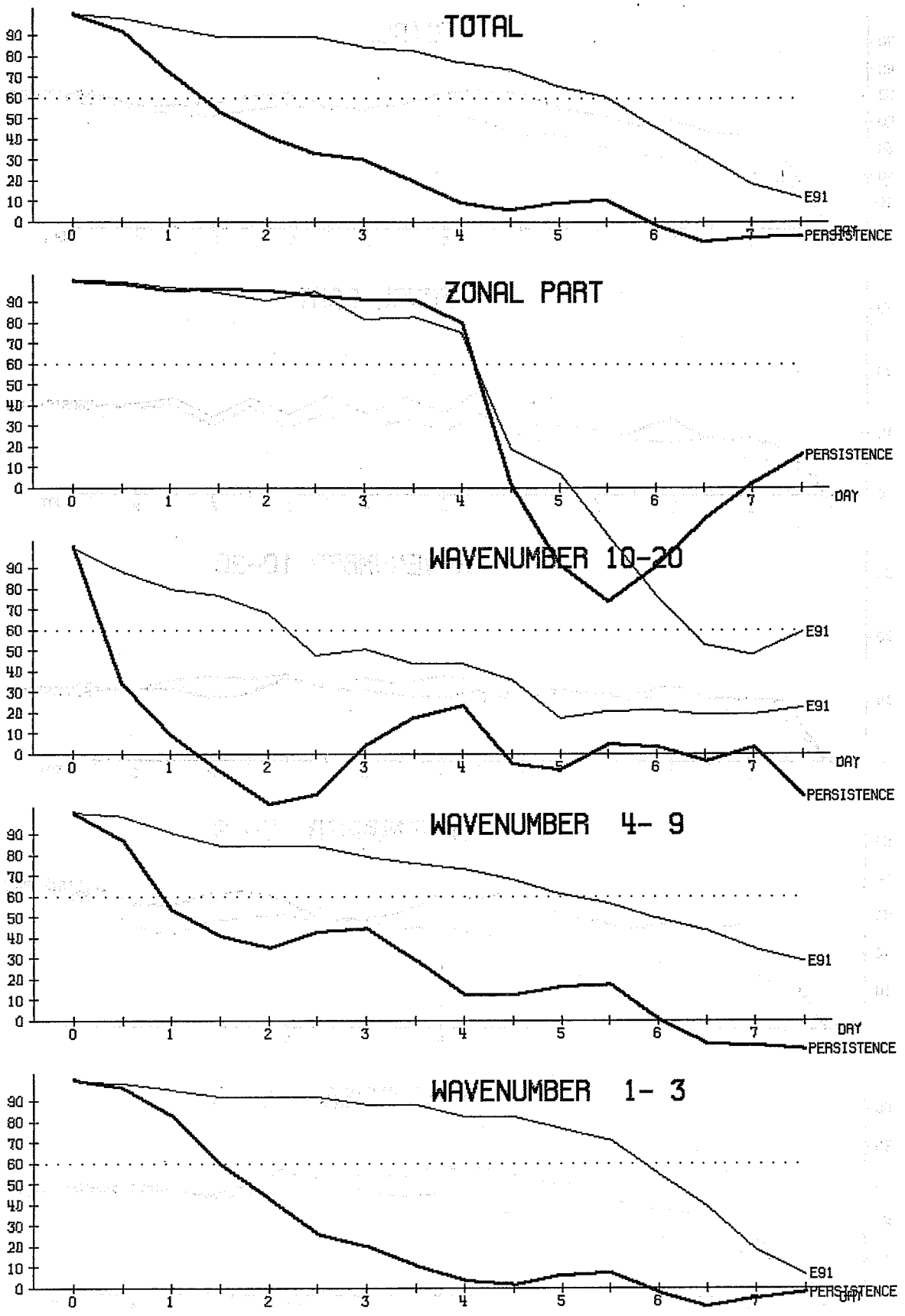

Fig. 14 E91 Anomaly correlation coefficients of the 500 mb. height fields

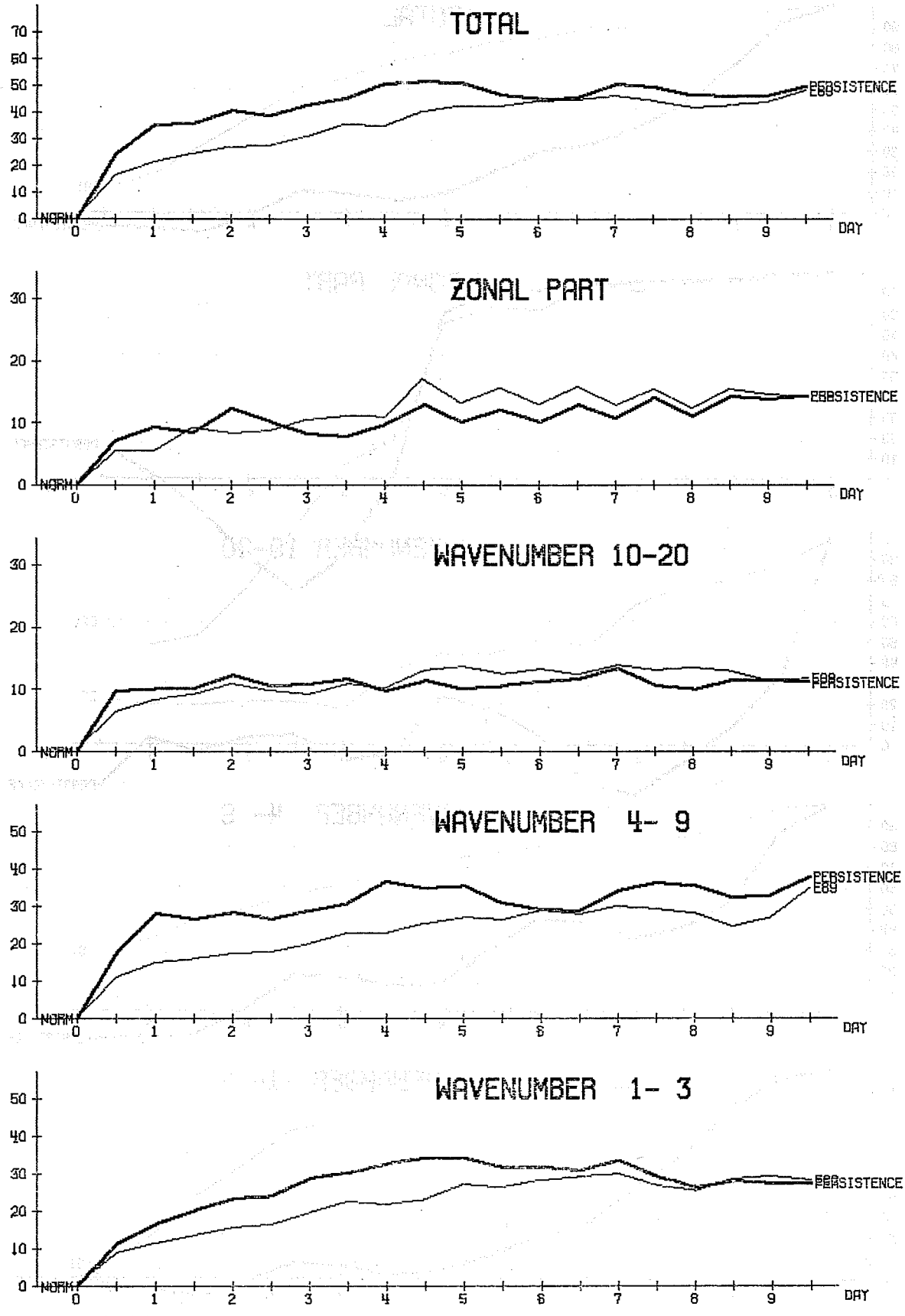

Fig. 15 E89 Mean standard deviation of the 850 mb temperature fields

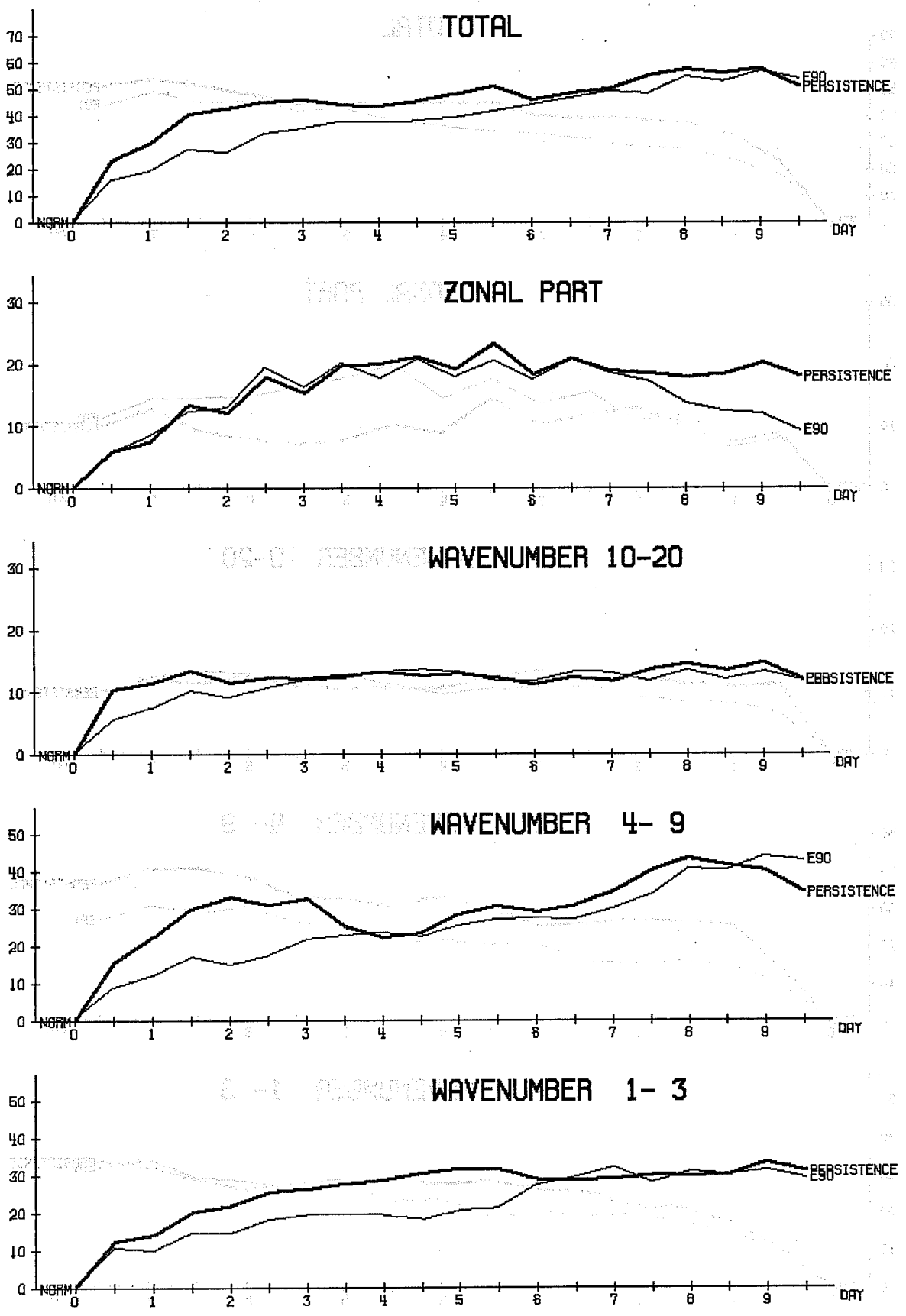

Fig. 16 E90 Mean standard deviation of the 850 mb temperature fields

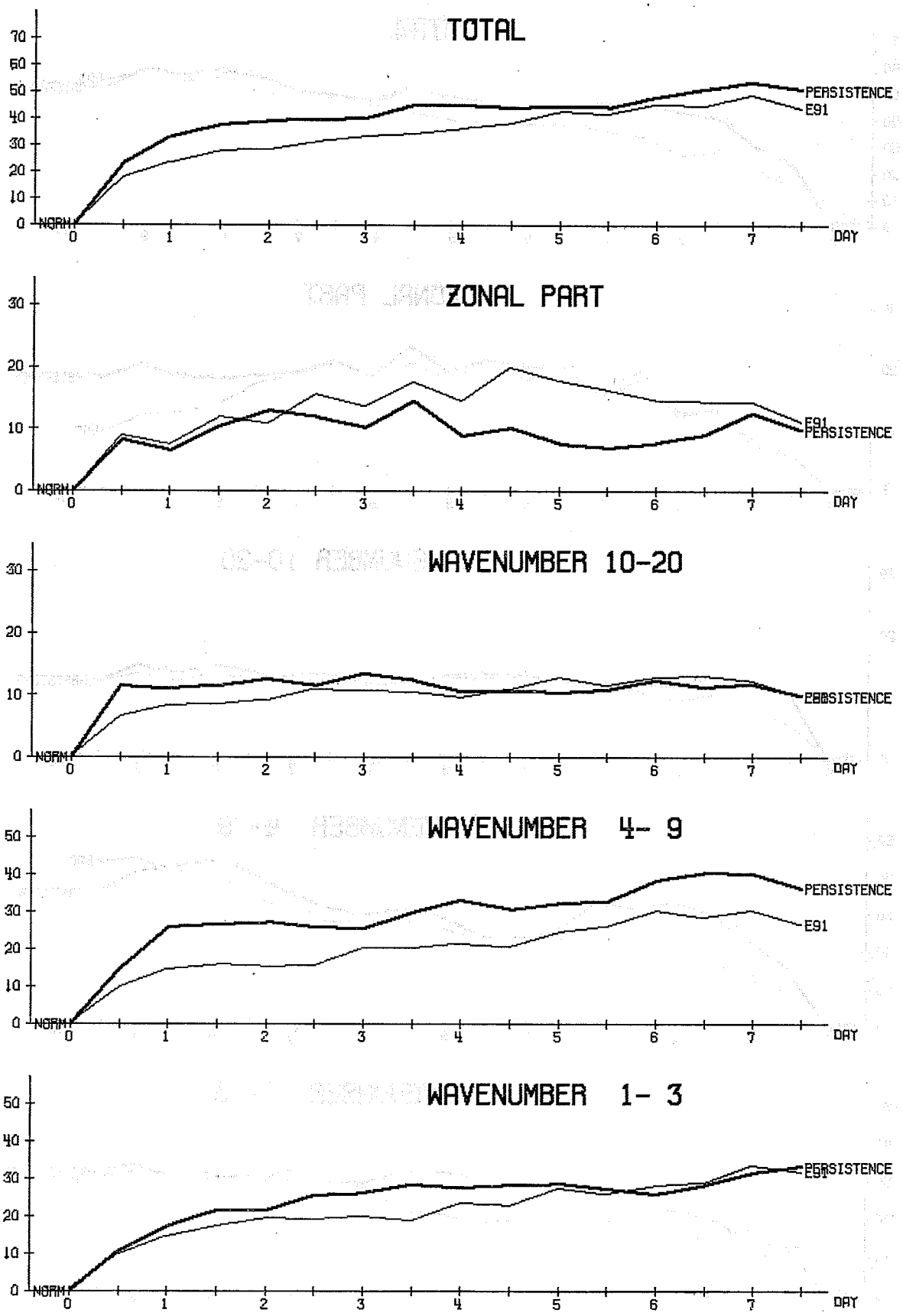

Fig. 17 E91 Mean standard deviation of the 850 mb temperature fields

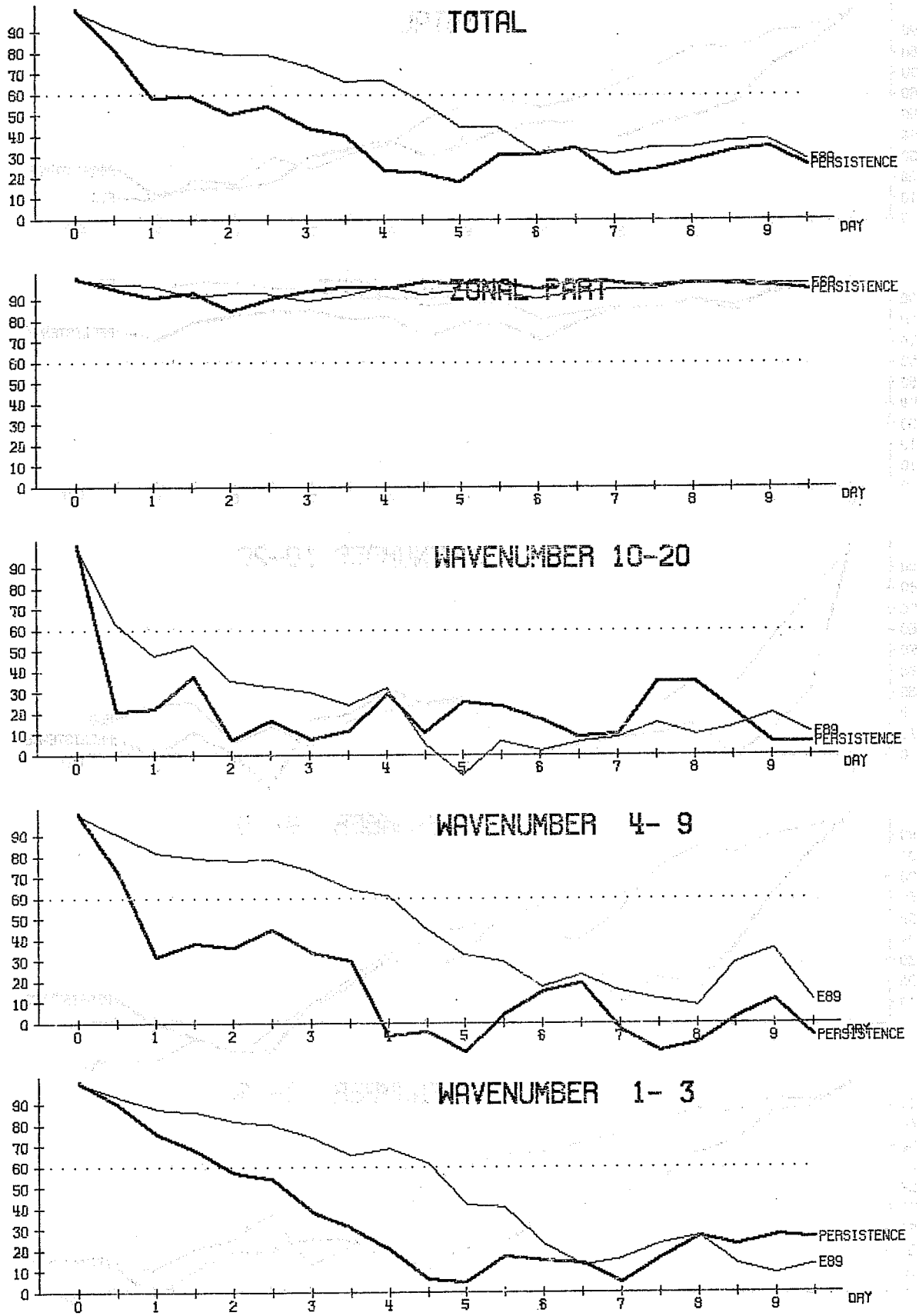

Fig. 18 E89 Anomaly correlation coefficients of the 850 mb temperature fields

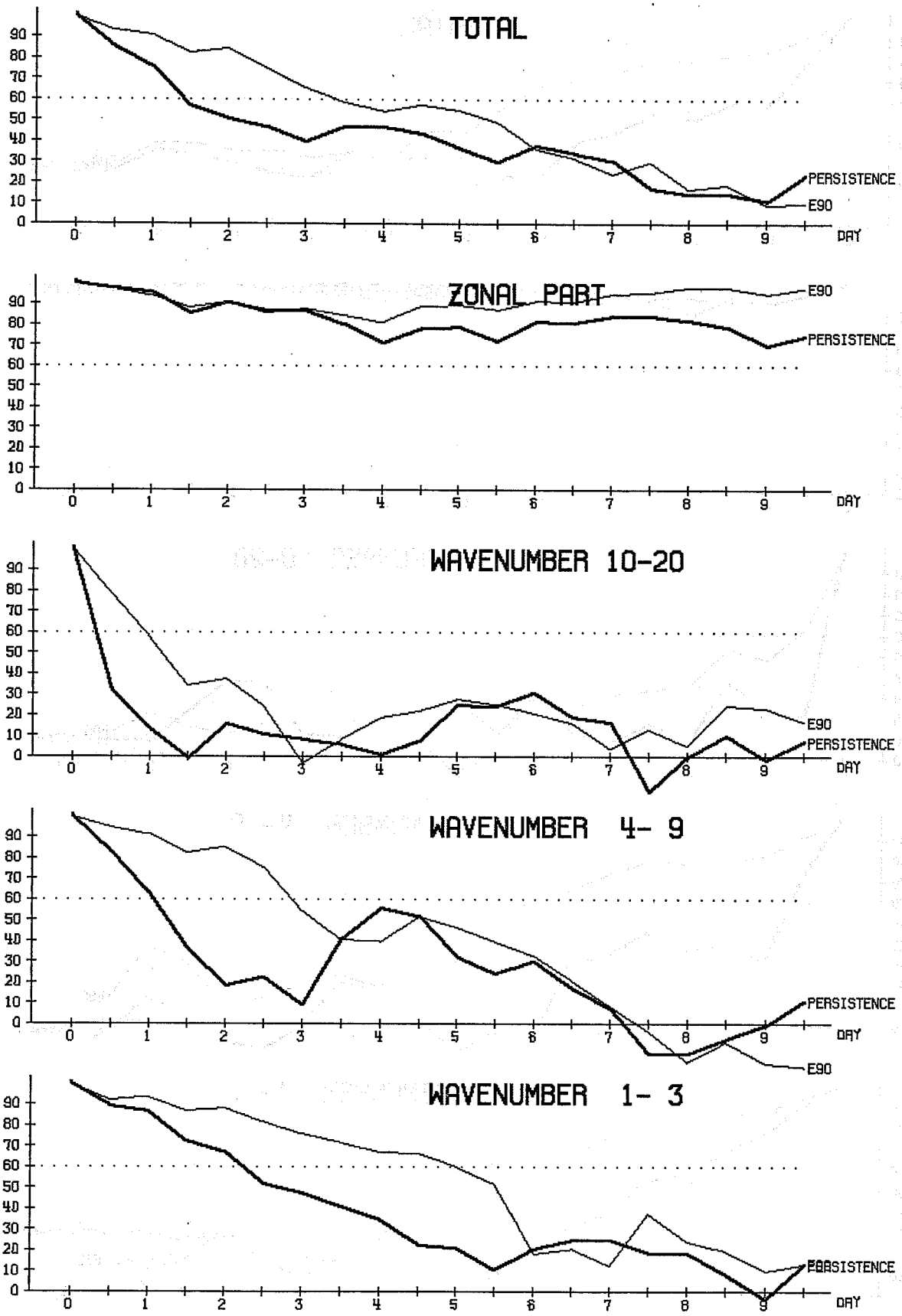

Fig. 19 E90 Anomaly correlation coefficients of the 850 mb temperature fields

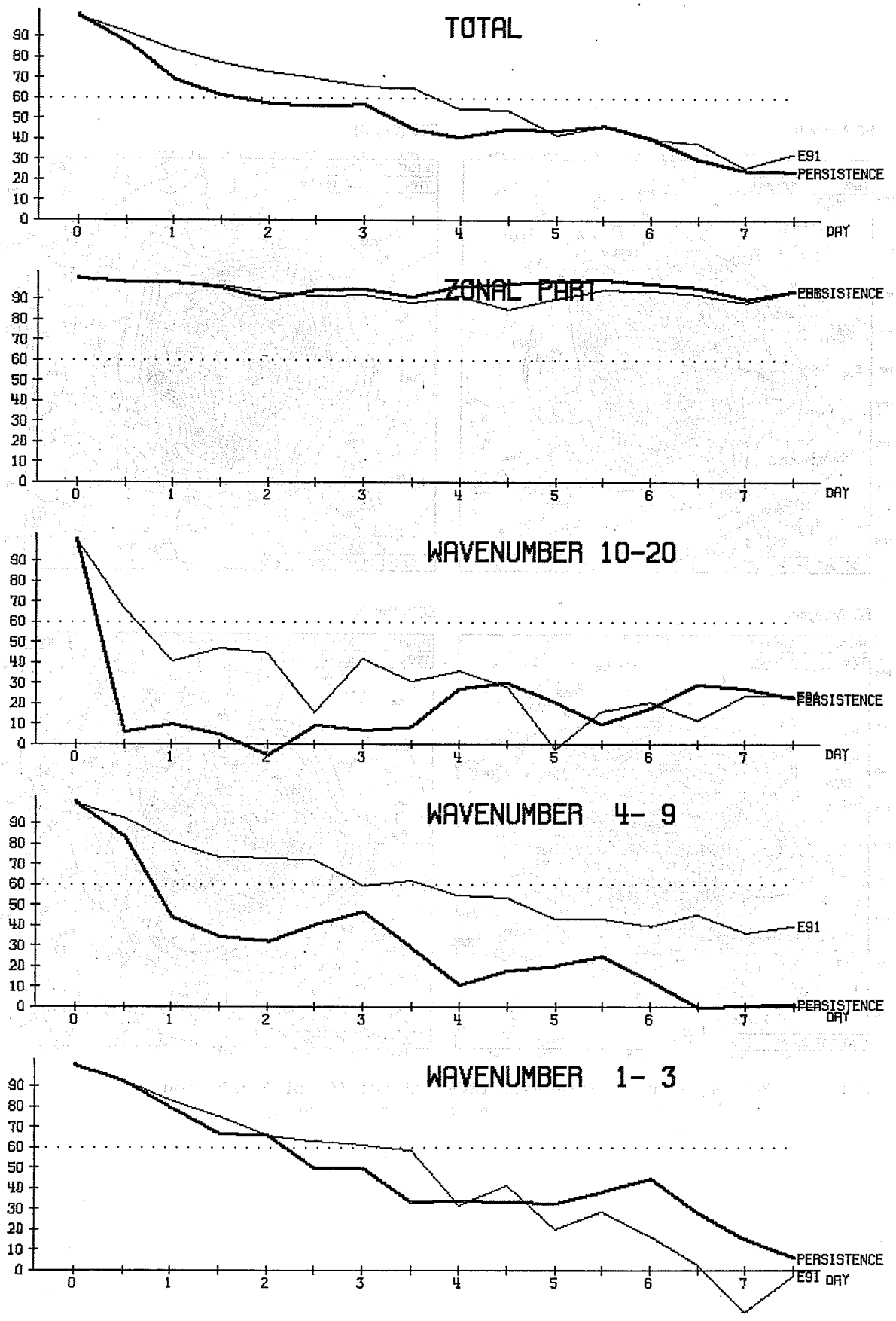

Fig. 20 E91 Anomaly correlation coefficients of the 850 mb temperature fields

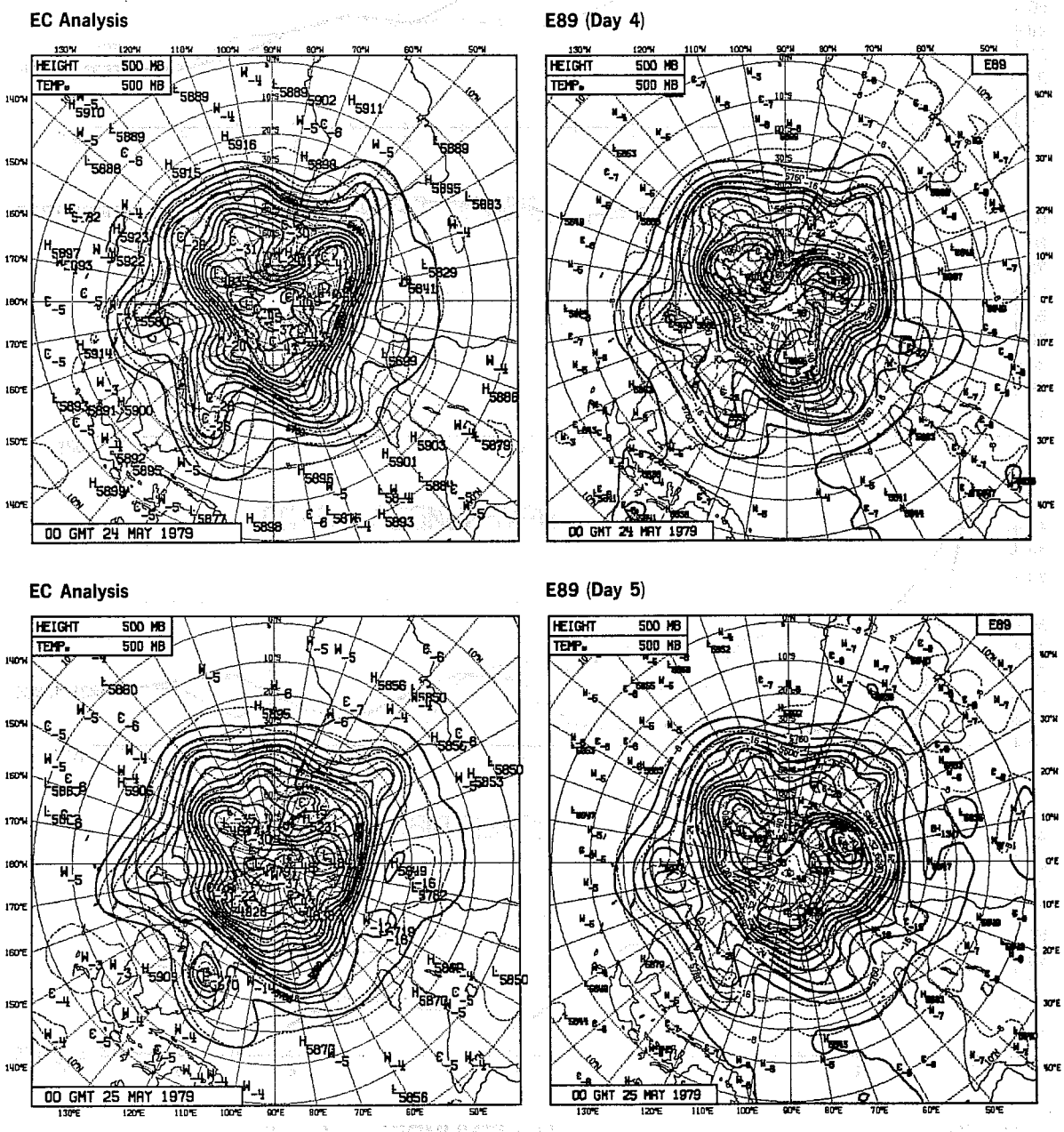

Fig. 21 E89 Day 4 and 5 forecasts (E89) of the 500 mb height and temperature fields with the corresponding analyses

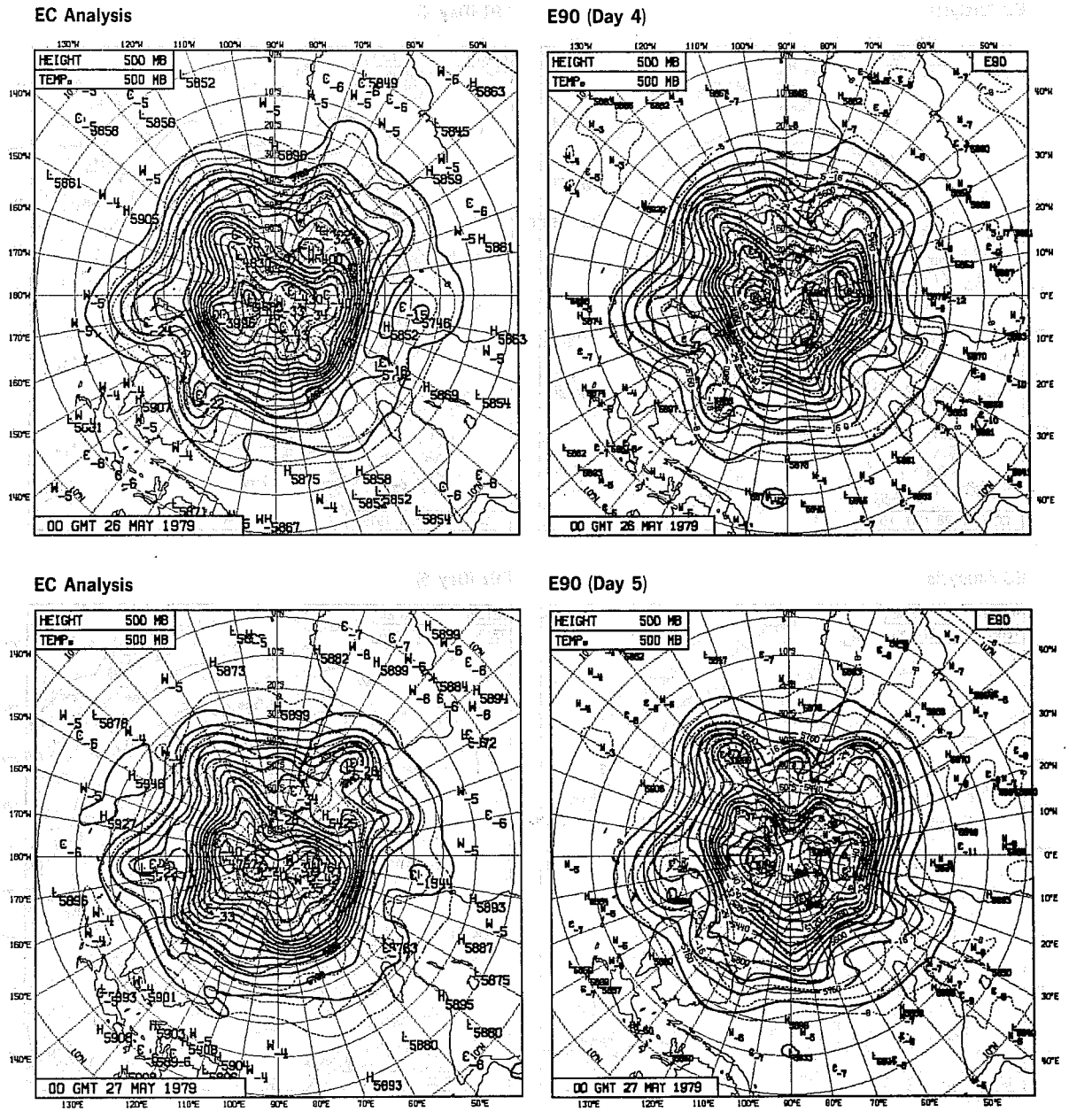

Fig. 22 E90 Day 4 and 5 forecasts (E90) of the 500 mb height and temperature fields with the corresponding analyses

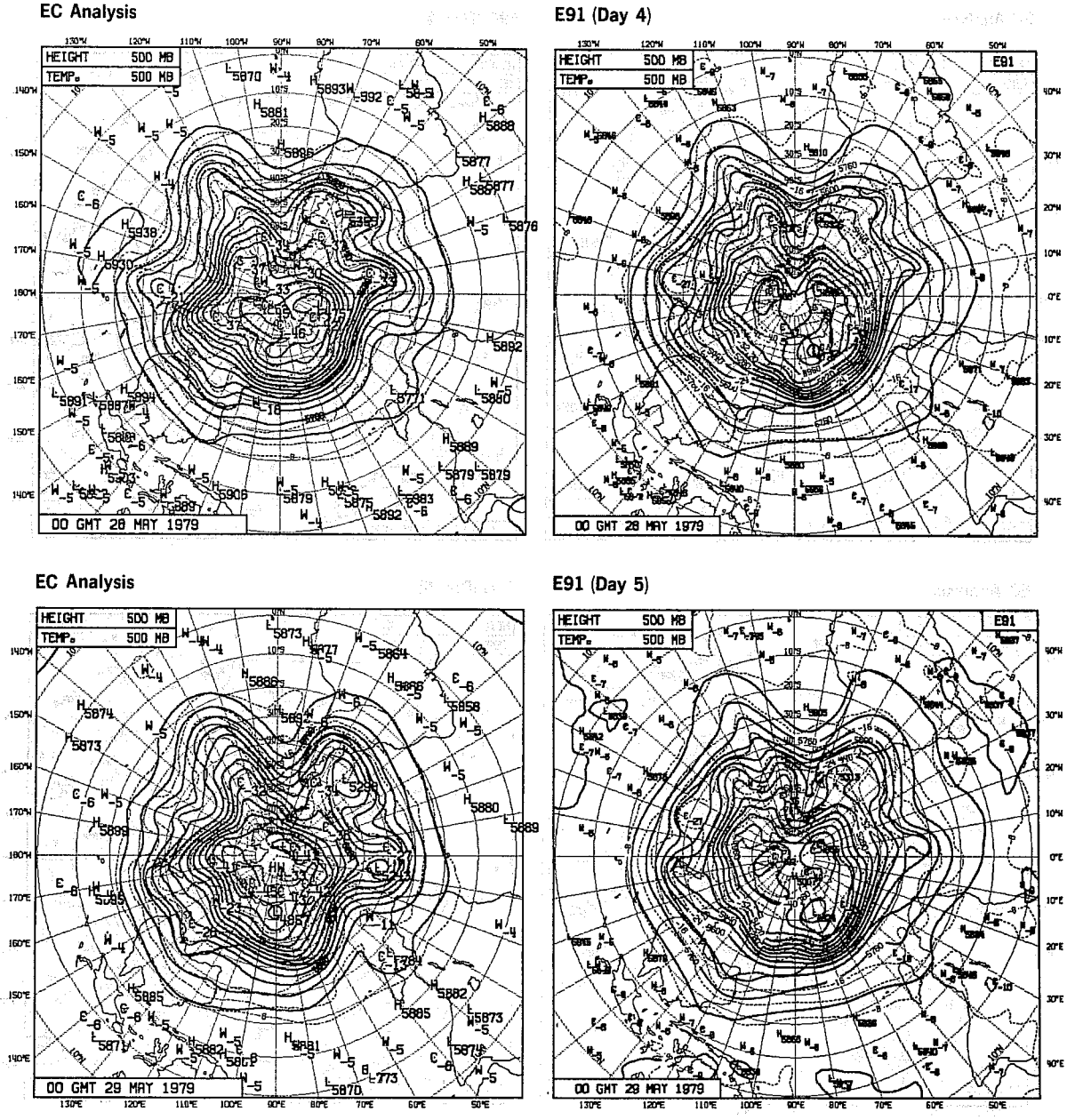

Fig. 23 E91 Day 4 and 5 forecasts (E91) of the 500 mb height and temperature fields with the corresponding analyses